ISSN 1996-3343

Asian Journal of Applied Sciences

http://knowledgiascientific.com

Knowledgia SCIENTIFIC
A Place to Publish Outstanding Research

Asian Journal of Applied Sciences 4 (2): 137-154, 2011
ISSN 1996-3343 / DOI: 10.3923/ajaps.2011.137.154

Numerical Study of the Natural Ventilation in House: Cases of Three Rectangular Scale Models

[1]Augustin Memeledje, [2]Maurice Djoman, [1]Alhassane Fofana, [2]Aboudramane Gbané and [1]Aboubakar Sako

[1]Laboratoire de Physique de l'atmosphère et mécanique de fluides UFR-SSMT Université d'Abidjan Cocody, 22 BP 582 Abidjan 22, Côte d'Ivoire

[2]Laboratoire d'Energie Solaire, UFR-SSMT Université d'Abidjan Cocody, 22 BP 582 Abidjan 22, Côte d'Ivoire

Corresponding Author: Augustin Memeledje, 22 BP195 Abidjan 22, Côte d'Ivoire Tel: (225) 22 48 38 38, 225 07 28 77 20

ABSTRACT

In a rectangular room of scale model, we have simulated the turbulent airflows in two dimensions. These simulations have aimed to determine dynamic and thermal fields with a view to do recommendations to realize the natural ventilation in a room to reach a sufficient thermal comfort. Three simulations have being performed in following order in the different configurations: C12, C13 and C23. The results of those have seemed to show difficulties to ventilate the room. These difficulties proceeded from the incapability to guide air at will. So, we have noticed that the level of velocity was feeble in central regions which were often occupied in a room.

Key words: Natural ventilation, numerical simulation, dynamic field, thermal field, extraction

INTRODUCTION

The thermal comfort in house dealt with in many studies (Ziskind *et al*., 2002; De Dear and Braer, 2002; Memeledje *et al*., 2006, 2010); however today, it often gives rise to an interest for reasons of economy energy and of productivity depending on the user's health. In tropical areas, the thermal comfort is often obtained by air-conditioning apparatus. However, these last years, the dearness of energy encouraged or favoured different searches of natural ventilation in scale models (Da Graca *et al*., 2002) and buildings (Sacre *et al*., 1992; Sangkertadi, 1994). So, we tried to purpose, in scale model an approach to realize the ventilation. The realization of the comfort without air-conditioning is very worrying when interior ambiences of houses are very hot. This state is more felt in absence of airflow. In these works, our researched aim is not to study different energies balances, but only to try to apprehend airflows distributions in a room to reach natural ventilation when extraction is produced at the ceiling.

FLOW MODELLING

Mathematical modelling: In turbulent state, we study airflow in a rectangular room. This flow is due to density variations in volume forces and extraction forces at the ceiling. It is described in steady state, incompressible conditions without wells or substance sources or internal heat sources. For a physical property ϕ, in two-dimensional Cartesian representation, the conservation equations (Rodi, 1980), in unsteady state, are generally expressed as:

$$\frac{\partial \rho \Phi}{\partial t} + \frac{\partial (\rho U \Phi)}{\partial x} + \frac{\partial (\rho V \Phi)}{\partial y} = \frac{\partial}{\partial x}\left(\Gamma_{\Phi} \frac{\partial \Phi}{\partial x}\right) + \frac{\partial}{\partial y}\left(\Gamma_{\Phi} \frac{\partial \Phi}{\partial y}\right) + S_{\Phi} \quad (1)$$

This generic form gives a system of different partial differential equations following results as:

- **Mass conservation equation:**

$$\frac{\partial \rho}{\partial t} + \frac{\partial (\rho U)}{\partial x} + \frac{\partial (\rho V)}{\partial y} = 0 \quad (2)$$

- **Impulse conservation equation in x:**

$$\frac{\partial U}{\partial t} + \frac{\partial (UU)}{\partial x} + \frac{\partial (VU)}{\partial y} = \frac{\partial}{\partial x}\left((\nu + \nu_t) \frac{\partial U}{\partial x}\right) + \frac{\partial}{\partial y}\left((\nu + \nu_t) \frac{\partial U}{\partial y}\right) + \frac{1}{\rho} \frac{\partial P^*}{\partial x} \quad (3)$$

- **Impulse conservation equation in y Eq. 4:**

$$\frac{\partial V}{\partial t} + \frac{\partial (UV)}{\partial x} + \frac{\partial (VV)}{\partial y} = \frac{\partial}{\partial x}\left((\nu + \nu_t) \frac{\partial V}{\partial x}\right) + \frac{\partial}{\partial y}\left((\nu + \nu_t) \frac{\partial V}{\partial y}\right) + \frac{1}{\rho} \frac{\partial P^*}{\partial y} + g\beta(T - T_0) \quad (4)$$

- **Enthalpy conservation equation:**

$$\frac{\partial T}{\partial t} + \frac{\partial (UT)}{\partial x} + \frac{\partial (VT)}{\partial y} = \frac{\partial}{\partial x}\left((a + \frac{\nu_t}{\sigma_T}) \frac{\partial T}{\partial x}\right) + \frac{\partial}{\partial y}\left((a + \frac{\nu_t}{\sigma_T}) \frac{\partial T}{\partial y}\right) \quad (5)$$

- **Turbulent energy conservation equation:**

$$\frac{\partial k}{\partial t} + \frac{\partial (Uk)}{\partial x} + \frac{\partial (Vk)}{\partial y} = \frac{\partial}{\partial x}\left((\nu + \frac{\nu_t}{\sigma_k}) \frac{\partial k}{\partial x}\right) + \frac{\partial}{\partial y}\left((\nu + \frac{\nu_t}{\sigma_k}) \frac{\partial k}{\partial y}\right) + P_k + G - \varepsilon \quad (6)$$

where, production term (P_k) is given by:

$$P_k = \nu_t[(\frac{\partial U}{\partial x})^2 + (\frac{\partial V}{\partial y})^2 + \frac{1}{2}(\frac{\partial U}{\partial y} + \frac{\partial V}{\partial x})^2] \quad (7)$$

Destruction-production term (G) is calculated by the following Eq. 8:

- **Near of vertical wall:**

$$G = \beta g \frac{\nu_t}{\sigma_T}(\frac{\partial T}{\partial x}) \quad (8a)$$

- **Near of horizontal wall:**

$$G = \beta g \frac{\nu_t}{\sigma_T}\left(\frac{\partial T}{\partial y}\right) \tag{8b}$$

- **Dissipative energy conservation Eq. 9:**

$$\frac{\partial \varepsilon}{\partial t} + \frac{\partial (U\varepsilon)}{\partial x} + \frac{\partial (V\varepsilon)}{\partial y} = \frac{\partial}{\partial x}\left(\left(\nu + \frac{\nu_t}{\sigma_\varepsilon}\right)\frac{\partial \varepsilon}{\partial x}\right) + \frac{\partial}{\partial y}\left(\left(\nu + \frac{\nu_t}{\sigma_\varepsilon}\right)\frac{\partial \varepsilon}{\partial y}\right) + C_{1\varepsilon}\frac{\varepsilon}{k}\left(P_k + C_{3\varepsilon}G\right) - C_{2\varepsilon}\frac{\varepsilon^2}{k} \tag{9}$$

where, $c_{1\epsilon}$, $c_{2\epsilon}$, $c_{3\epsilon}$, c_μ, σ_T, σ_ϵ and σ_k are turbulence constants.

For this study, the adopted constants are those of standard model: $c_{1\epsilon} = 1.14$, $c_{2\epsilon} = 1.92$, $c_{3\epsilon} = 1$, $c_\mu = 0.09$, $\sigma_T = 1$, $\sigma_\epsilon = 1.3$, $\sigma_k = 1$.

Numerical modelling: The transport diffusion Eq. 1 is integrated by numerical technique. The discretization was performed using the mesh method described by Patankar (1980). The method uses three shifted meshes for the variable described in dynamic and thermal fields (Fig. 1). The scalar variables (P, T, k, ϵ) are determined for points (p) located in the principal mesh (1), where E, W, N, S are respectively the cardinal locations East, West, North, South. So, the integration on the principal control volume gives this expression:

$$A_P\Phi_P = A_{PE}\Phi_E + A_{PW}\Phi_W + A_{PN}\Phi_N + A_{PS}\Phi_S + B_{P\Phi} \tag{10}$$

As for the horizontal and vertical components U and V of the velocity, they are respectively determined in the two secondary meshes Eq. 2 and 3, where the orientations are given by e and n; secondary mesh Eq. 2 centred on (e) gives horizontal velocity U_e:

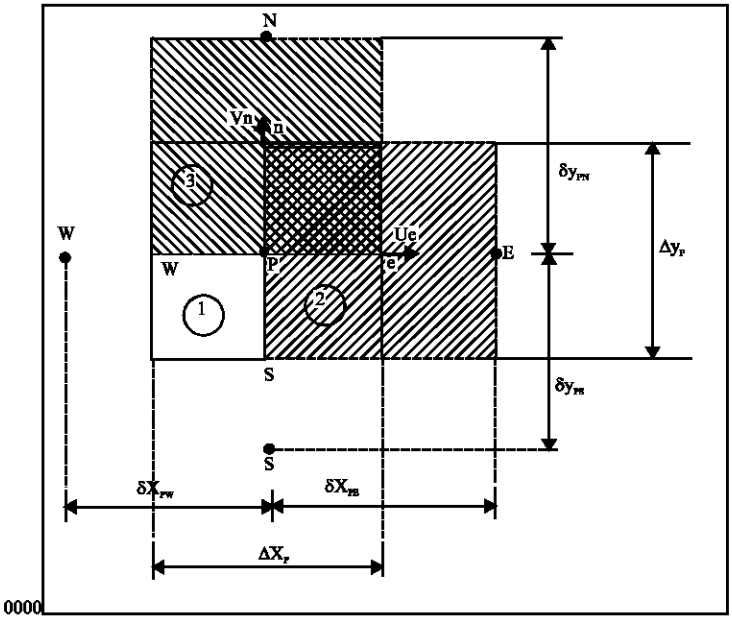

Fig. 1: Representation of 3 control volumes

$$A_eU_e = A_{eE}U_{eE} + A_{eW}U_{eW} + A_{eN}U_{eN} + A_{eS}U_{eS} + Bu_e \quad (11)$$

where:

$$Bu_e = B_{eU} + d_{ue}(P_p - P_E) \quad (12)$$

secondary mesh Eq. 3 centred on (n) determines vertical velocity V_n:

$$A_nV_n = A_{nE}V_{nE} + A_{nW}V_{nW} + A_{nN}V_{nN} + A_{nS}V_{nS} + Bv_n \quad (13)$$

where:

$$Bv_n = B_{nv} + d_{vn}(P_p - P_N) \quad (14)$$

du_e and dv_n are the coupling coefficient between velocity and pressure fields by the Eq. 12 and 14. The coefficients A in the correlations Eq. 10, 11 and 13 are calculated with the help neighbouring cardinal points (E, W, N and S) round unknowns U, V, P, T, k and ϵ.

Afterwards, these linear integrated equations on respective meshes lead to a system of finite difference equations expressed as:

$$A_i\Phi_i = \sum A_{ij}\Phi_j + B_{\Phi i} \quad (15)$$

$$B_{\Phi i} = S_{\Phi i}\left(\frac{\Delta x_i \Delta y_i}{\Delta t}\right) \quad (16)$$

where, B_Φ represents sources terms of Φ_i; the coefficients A_i and A_{ij} are respectively calculated by the following formulas according to the type of variable (scalar or vector):

$$A_i = \rho\frac{\Delta x_i \Delta y_i}{\Delta t} + F_{Ci} + \Sigma A_{ij} \quad (17)$$

$$A_{ij} = D_j A\left(\left|Pe_j\right|\right) + \mathrm{Max}\left(\pm F_j, 0\right) \quad (18)$$

where, $A(|Pe_j|)$ is a function of Peclet number (Pe_j) which is the ratio between convection and local diffusion. It depends on the adopted scheme. In this calculation, we have chosen the hybrid scheme. This scheme used the following relation:

$$A\left(\left|Pe_j\right|\right) = \mathrm{Max}\left(0.1 - 0.5\left|Pe_j\right|\right)$$

where, $Pe_j \leq 2$ and $Pe_j > 2$. Moreover F_j takes the sign (-) when a convective flux is going out a control volume and (+) when it is entering it. F_{Ci} is the mass default of the mesh around a node i; for example, for the principal grid (E, W, N, S) around a point (p):

$$F_{CP} = \left(\rho U_e \Delta y_p - \rho U_W \Delta y_p\right) + \left(\rho V_n \Delta x_p - \rho V_s \Delta x_p\right) \quad (19)$$

Table 1: Boundary conditions

	Lateral wall South	Lateral wall North	Floor	Ceiling	Admission orifice	Extraction orifice	Symmetry conditions
U (m sec^{-1})	0	0	0	0	U known by continuity	0	0
V (m sec^{-1})	0	0	0	0	0	V = 0.45	$\frac{\partial V}{\partial n} = 0$
P'	$\frac{\partial P'}{\partial n} = 0$	$\frac{\partial P'}{\partial n} = 0$	$\frac{\partial P'}{\partial n} = 0$	$\frac{\partial P'}{\partial n} = 0$	$\frac{\partial P'}{\partial n} = 0$	$\frac{\partial P'}{\partial n} = 0$	$\frac{\partial P'}{\partial n} = 0$
T(°C)	$T_{ps} = 29.5$	$T_{pn} = 29.5$	$\frac{\partial T}{\partial n} = 0$	$\frac{\partial T}{\partial n} = 0$	$T_e = 24$	$\frac{\partial T}{\partial n} \neq 0$	$\frac{\partial T}{\partial n} \neq 0$
k	k = 0	k = 0	k = 0	k = 0	$\frac{\partial k}{\partial n} = 0$	$\frac{\partial k}{\partial n} = 0$	$\frac{\partial k}{\partial n} = 0$
ϵ	$\frac{\partial \varepsilon}{\partial n} = 0$	$\frac{\partial \varepsilon}{\partial n} = 0$	$\frac{\partial \varepsilon}{\partial n} = 0$	$\frac{\partial \varepsilon}{\partial n} = 0$	$\frac{\partial \varepsilon}{\partial n} = 0$	$\frac{\partial \varepsilon}{\partial n} = 0$	$\frac{\partial \varepsilon}{\partial n} = 0$

Note that for closing the system of five equations with five unknowns.

One supplementary equation has been added to separate pressure and velocity fields. This equation is linearly expressed as:

$$A_{pp} P'_{\rho} = A_{Ep} P'_{E} + A_{wp} P'_{W} + A_{Np} P'_{N} + A_{Sp} P'_{s} + B_{pp} \quad (20)$$

where, P' is the variable correction of pressure; the new estimated value of pressure is P+P'. This last value is estimated until that convergence is reached. The separation (pressure-velocity) is obtained by the algorithm SIMPLE (Semi-Implicit Method for Pressure Linked Equation). To solve this equation, the Alternating Direction Implicit (ADI) method is used on the representation with three successive nodes (Dainese, 1994; Estivalez, 1989). Consequently, by the Eq. 15, we have obtained a system of 6 non linear equations with Eq. 6 unknowns (U, V, P, T, k, ϵ). This studied field has been meshed into a regular grid with (60.60) measure points.

Boundary conditions: The boundary conditions are given in Table 1 for non symmetrical and symmetrical studies. This Table presents Dirichlet and Newman conditions according to the type of studied configurations. Three configurations have been defined:

- **C12:** One admission orifice (in lateral wall) and two extraction orifices (in ceiling) (non symmetrical study)
- **C13:** One admission orifice (in lateral wall) and three extraction orifices (in ceiling) (non symmetrical study)
- **C23:** Two admission orifices (in lateral wall) and three extraction orifices (in ceiling) (symmetrical study)

Moreover, for a calculation in regular grid and to avoid solving neighbouring wall fluid layers, wall functions were adopted (Brunet, 1989) such as:

$$\text{For } 0 < Y^+ \leq 11.5, \qquad U^+ = Y^+ \qquad \text{where, } Y^+ = \frac{U_*}{\nu} Y$$

$$\text{For } 11.5 < Y^+ \leq 100, \qquad U^+ = \frac{1}{\kappa} \text{Ln} C_e Y^+$$

where, Y^+ and U^+ are respectively dimensionless variable and velocity.

For $30 < Y_0^+ \leq 100$, we adopted:

- **Turbulent energy:**

$$k_0 = \frac{U_*^2}{\sqrt{C_\mu}}$$

- **Dissipative energy:**

$$\varepsilon_0 = \frac{U_*^3}{\kappa Y_0}$$

where, U_* is the friction velocity and κ is Von Karman constant, κ=0.41.

VALIDATION AND TEST PROCEDURE

This validation has been done in a symmetrical model (Memeledje, 1998, 2007) named C22 configuration (2 admission orifices and 2 extraction orifices). Here, we compared two dynamic profiles [theoretical (numerical simulation results) and experimental] between two distinct regions as shown on (Fig. 2); we also compared two thermal profiles:

- The Lower Region (LR), defined by position 4.8 cm
- The Higher Region (HR), characterised by position 84 cm

We have chosen these regions to avoid the very heavy instabilities that we have precisely noticed at the altitude 54 cm during the different measurements. These have respectively been performed by a fire file anemometer and a thermometric system. Last system, provided with a HP3421A scanner at 30 channels, gives different temperatures to ambience. It uses K thermocouple (K defines chromium-nickel and aluminium-nickel).

Each system is connected to an own microcomputer and makes measures at a distance in using cables.

After the calibration of these two systems, we have obtained following precisions:

- In a range of velocities (0 to 120 cm sec^{-1}), the absolute incertitude doesn't reaches 2 cm sec^{-1}
- In a range of temperatures (0 to 60°C), this incertitude doesn't exceed 0.3 K

The retained conditions for this validation are specified by mechanical extraction and room temperature condition; at the ceiling, mechanical extraction conditions were used:

- Mass rate flow: $\dot{m}_{ex} = 0.089$ kg sec^{-1}
- extraction velocity: $V_{ex} = 0.41$ m sec^{-1}
- Reynolds number in extraction orifice: Re = 5466, this last value indicates that flow is turbulent

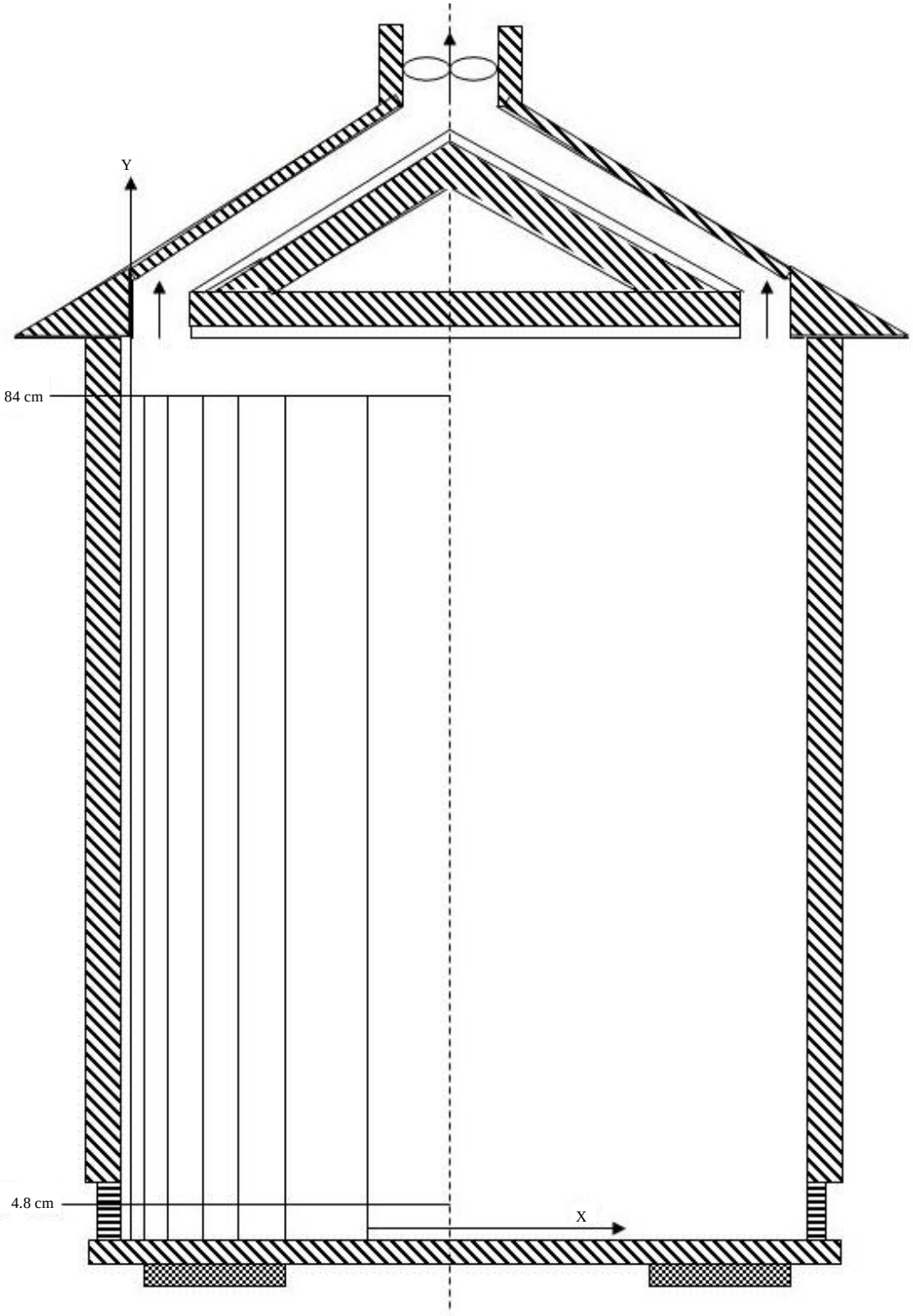

Fig. 2: Location of measure points

Room temperature conditions are characterized by two controlled walls (South and North wall) and two walls in natural evolution (ceiling and floor). The measurements performed respectively, in the lower regions (identified with letter L) and in the upper regions (with letter H) led to the following temperatures and their variations:

- **South wall temperatures:**

$$Tp_{sL} = 29.8°C,\ Tp_{sH} = 29.4°C,\ |Tp_{sL} - Tp_{sH}| = 0.4°C$$

- **North wall temperatures:**

$$Tp_{nL} = 32.1°C,\ Tp_{nH} = 32.8°C,\ |Tp_{nL} - Tp_{nH}| = 0.7°C$$

- **Ceiling temperatures:**

$$Tc_{L} = 22.4°C,\ Tc_{H} = 22.0°C,\ |Tc_{L} - Tc_{H}| = 0.4°C$$

- **Floor temperatures:**

$$Tf_{L} = 21.7°C,\ Tf_{H} = 21.0°C,\ |Tf_{L} - Tf_{H}| = 0.7°C$$

- **Room central region (air temperature):**

$$Ta_{L} = 23.2°C,\ Ta_{H} = 21.0°C,\ |Ta_{L} - Ta_{H}| = 2.2°C$$

It can be observed that the temperature variations between lower and upper regions are very small for walls excepted air temperature variation that reaches 2.2°C. We can suppose that this variation cannot modify appreciably different velocity fields when study is done by mechanical extraction.

In lower regions (Y = 4.8 cm, Fig. 3), the temperature variation is 0.5°C between experimental and theoretical results; In upper regions (Y = 84 cm, Fig. 4), experimental and theoretical graphs

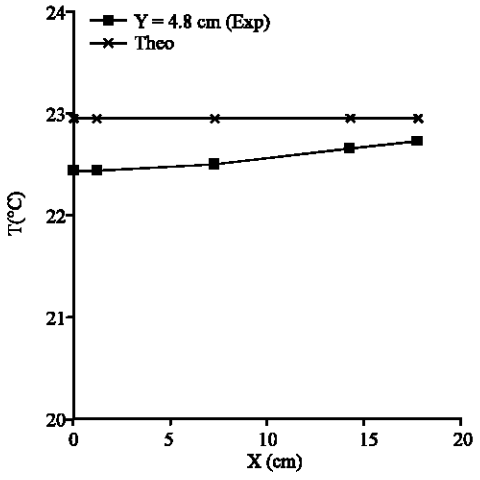

Fig. 3: Profiles of horizontal temperatures in Lower Region (LR)

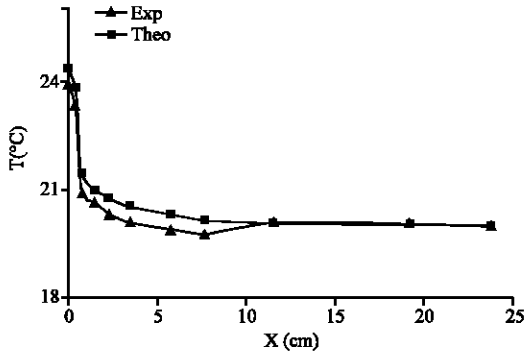

Fig. 4: Profiles of horizontal temperatures in Upper Region (HR)

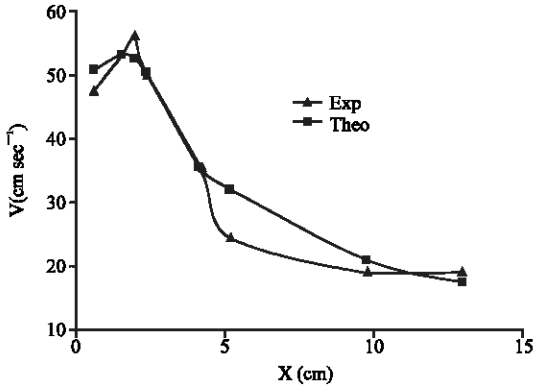

Fig. 5: Horizontal velocity distributions in Lower Region (LR)

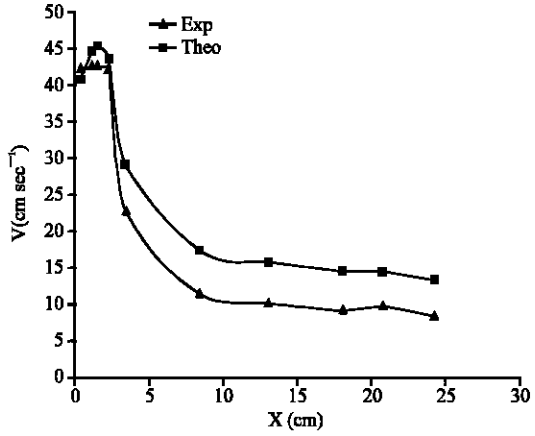

Fig. 6: Horizontal velocity distributions in Lower Region (HR)

are almost confounded. The velocity distributions (theory and experiment) have nearly the same graph in lower and upper regions. In lower regions (Y = 4.8 cm, Fig. 5), the velocity variation between theory and experiment is important, it almost reaches 10 cm sec^{-1} for x = 5 cm. In upper regions (Y = 84 cm, Fig. 6), this variation doesn't exceed to 10 cm sec^{-1} (maximum value). Main

reasons of velocity variations can be caused by the heavy fluctuations of turbulent flow and the quality of measurement by a fire file anemometer. This apparatus remains enough imprecise for low velocities.

Consequently, all the wall temperatures are considered to be roughly constant, with an error about 1°C. The results of this validation are, respectively given on Fig. 3 and 5 for the lower regions and Fig. 6 and 4 for the upper regions. On the whole, the results show a fairly good agreement between theory and experiment in view of the turbulent state of airflow.

NUMERICAL RESULTS

After the software validation, the three configurations were scrutinized. To this end, a set of boundary conditions were chosen (Table 1), including the entry temperature (Te), the lateral walls temperature (T_{pn} and T_{ps}) and the room air temperature (Tair); then the characteristic flow parameters and the heat transfer in the room were calculated. Moreover, for a temperature difference between lateral wall and air ΔT_{pa}=1.5°C, the following non dimensional numbers were considered:

- Rayleigh cavity number $Ra_{cav} = 2.10^8$,

for C12,

- Reynolds cavity number $Re_{cav} = 6882$
- Richardson cavity number $Ri_{cav} = 6$,

for C13 and C23,

- Reynolds cavity number $Re_{cav} = 8437$
- Richardson cavity number $Ri_{cav} = 4$

These numbers (Re_{cav}) indicate that the flow is turbulent and predominated by forced convection. As for the Nusselt cavity number $Nu_{cav} = 78$, it shows that convective transfers are more important than thermal conduction in the cavity.

For the different defined configurations, the numerical simulations were carried out that allowed to obtain the streamlines, the isovelocities and the isotherms; meanwhile the results of the C12 and C23 configurations are given by Fig. 7 and 8 because the C13 results are fairly identical with those of C12, excepted to the extraction orifice located the middle region of the ceiling.

For the C12 configuration, the streamlines (Fig. 7a) shows two stretched vortex along the vertical Y axis; they are located near the vertical south and north walls. The south vortex is smaller than the north one which is stretched all along the wall. The isovelocities (Fig. 7b) show that the high velocities are located near the walls. Far away from the walls, in the central zone, they become low and vary from 10 to 20 cm sec^{-1}. The isotherms contour (Fig. 7c) indicates heavy thermal variations near the walls especially in south wall, in the ceiling and the floor. The north wall is not well cooled. It can be seen that the central room region does not undergo sensitive thermal

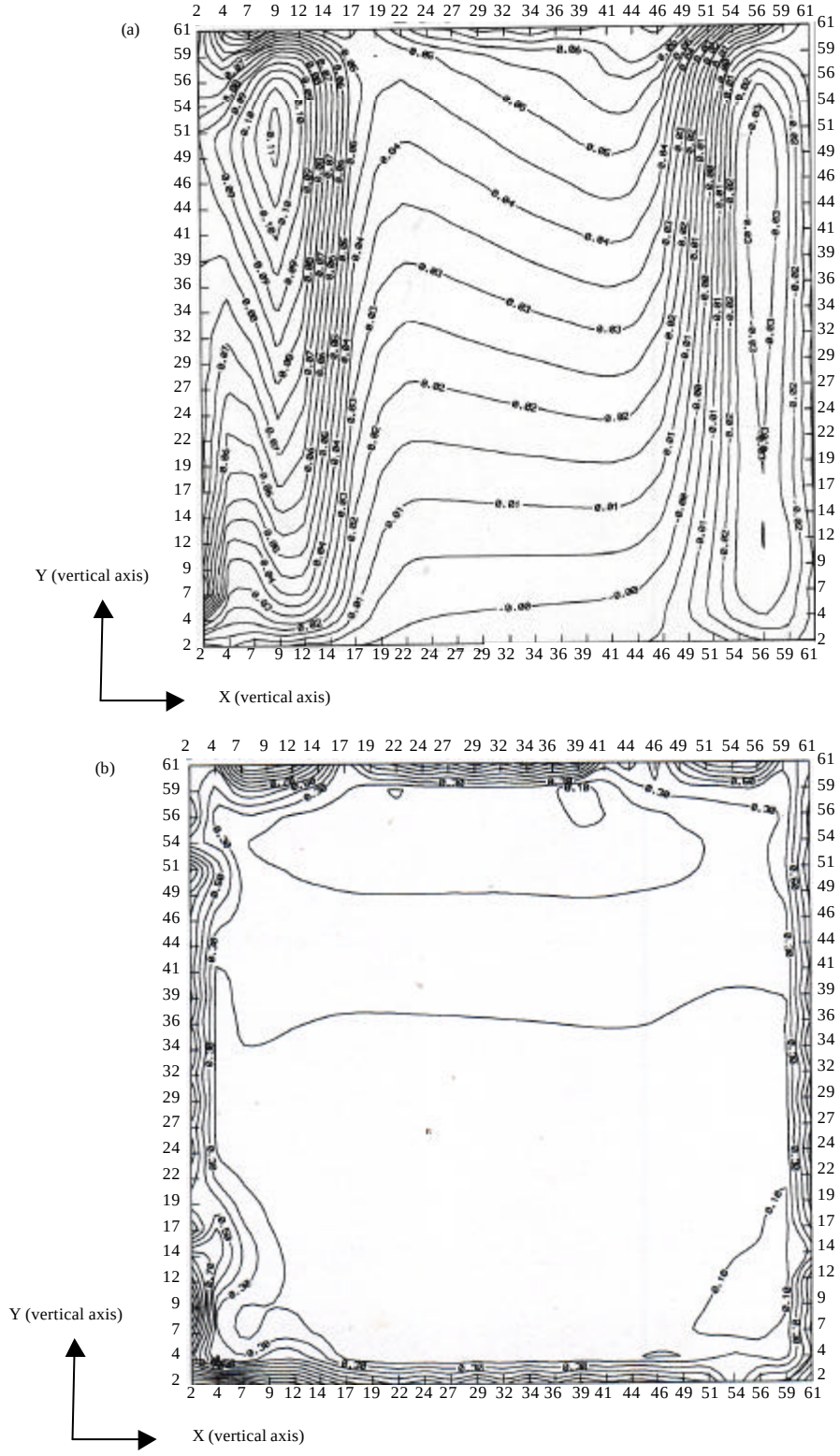

Fig. 7: Continued

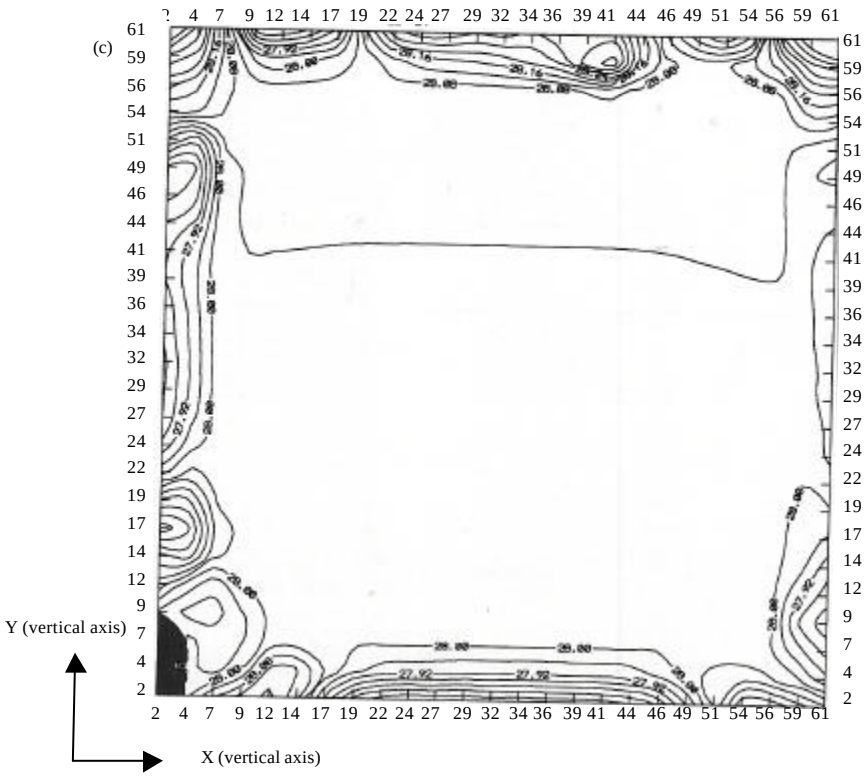

Fig. 7: (a) Streamlines C12 simulation, (b) isovelocities C12 simulation and (c) isotherms C12 simulation

modifications; this region has a uniform temperature (28°C). Consequently, the velocity levels of the central region are low, which does not create any thermal comfort. Then a new configuration (C13 configuration) was scrutinized. This configuration is adopted to lower the pressure in the ceiling middle, so that to increase the velocity levels in the central room regions and to cool the North wall.

For the same extraction velocity (0.45 m sec^{-1}) by ceiling orifice, C13 configuration shows that the dynamical and thermal fields are almost similar to those of C12 configuration.

Noticing that the neighbour regions of the north wall of C12 and C13 configurations do not undergo heavy thermal variations, the C23 configuration (Fig. 8) was simulated. In symmetrical study, it is noticed a stretched vortex along the vertical Y axis like in the configurations C12 and C13. In the same way, the heavy velocity variations are located near the walls, especially at the south wall and the ceiling (Fig. 8a). The central region has low velocities (Fig. 8b) which vary from 10 to 18 cm sec^{-1} approximately. The thermal field (Fig. 8c) shows a heavy thermal variation near by the south wall, the admission orifice and a low thermal variation near by the ceiling and the floor. A vertical thermal stratification is more sensitive in the central region. Moreover, the velocity distribution is more uniform in the central region than in the C12 configuration. Here the thermal field shows a heavy thermal variation near walls. The central regions have a uniform temperature (28.1°C). In this C23 configuration as previously observed for all the other configurations, the admission air temperature (24°C) does not especially influence the central regions.

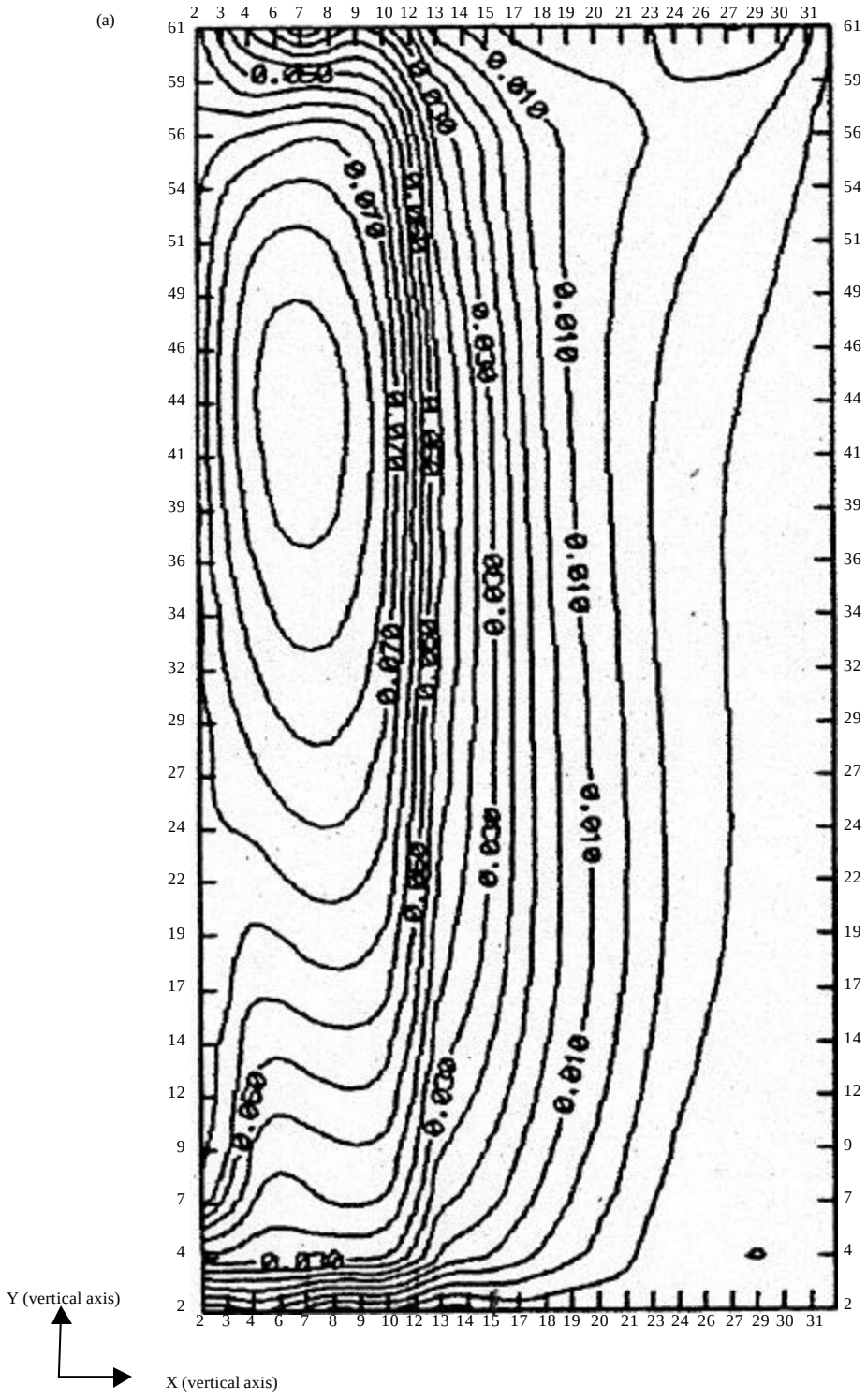

Fig. 8: Continued

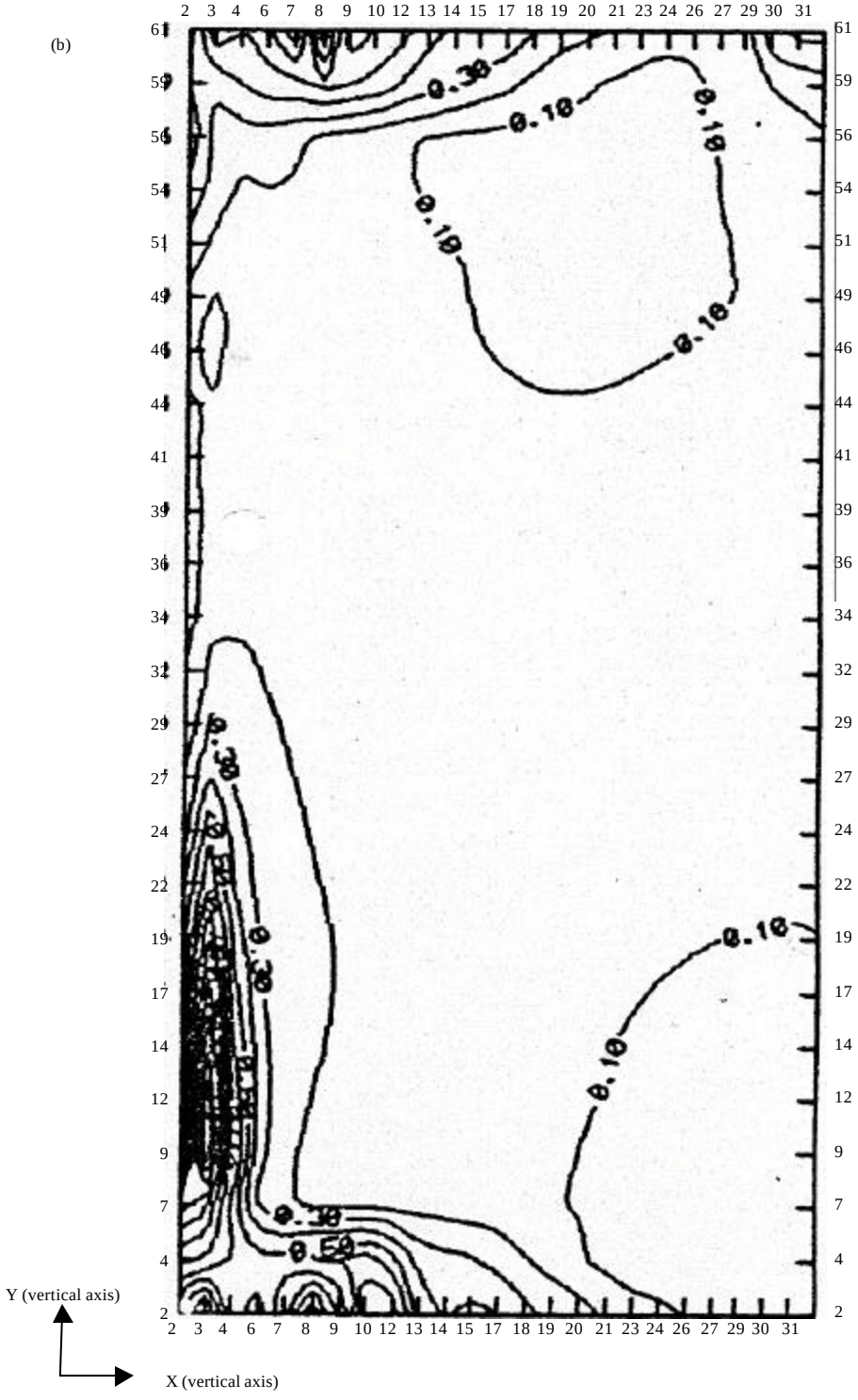

Fig. 8: Continued

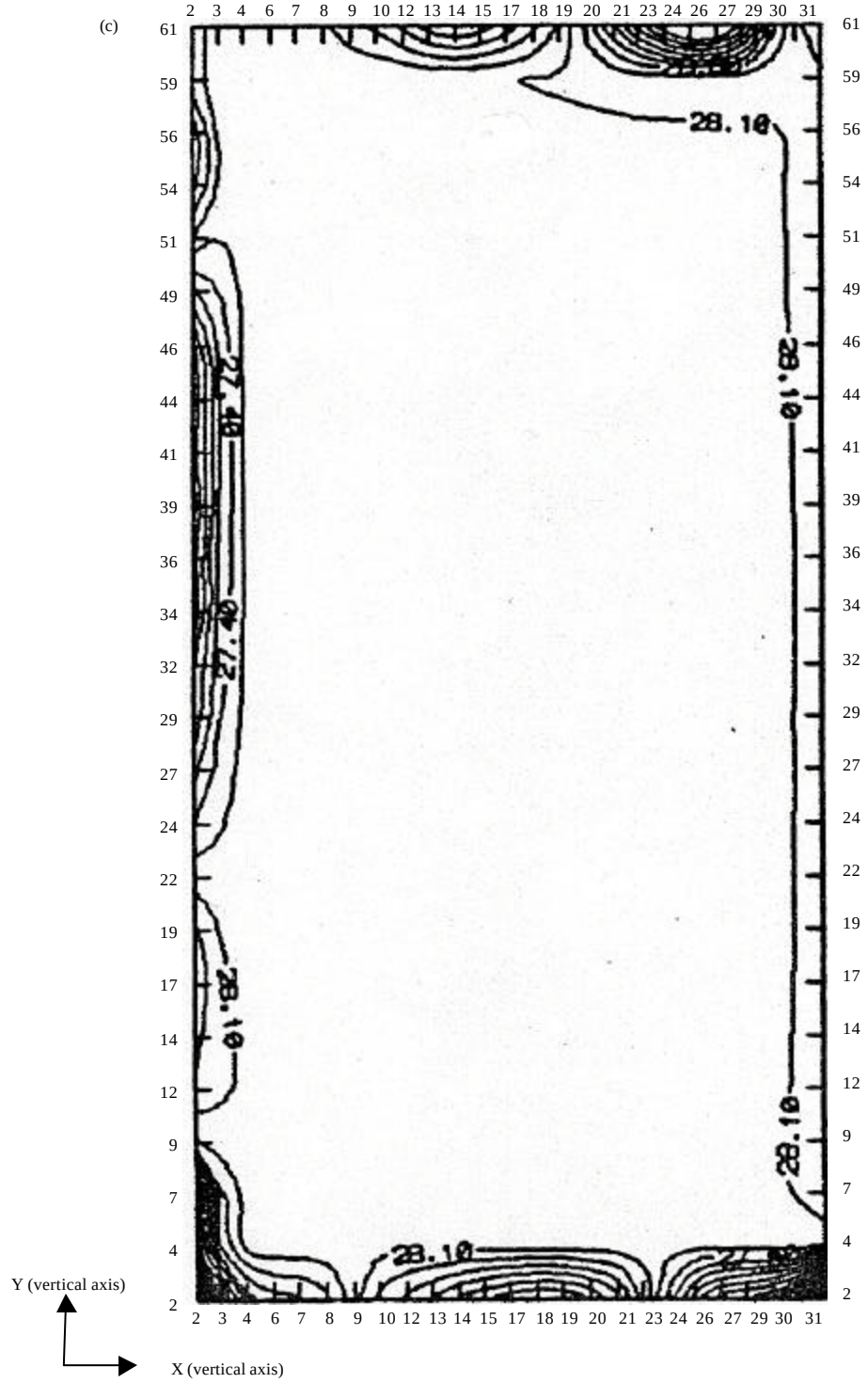

Fig. 8: (a) Streamlines C23 simulation, (b) isovelocities C23 simulation and (c) isotherms C23 simulation

CONCLUSIONS

The study undertaken in this paper by means of different simulations showed that if the orifices are not well positioned, the central region is not well fed by air flows. When air flows exist in this region, their velocities are low. None of the three configurations studied with the admission air temperature equal to 24°C at the bottom, allowed to create a sensitive thermal modification in the central region. The main thermal modifications are only observed all along the vertical wall. So this wall is the main thermal source of the room, its heat transfer can be used to stabilize enough the central region temperature during a free evolution. Hence, if this wall is kept at a constant temperature, convection effects can help to drop its temperature and so to reduce the thermal gain of the room. From the analysis of the three configurations, it can be stated that a cool air admission by the floor could be a solution to increase the velocity effects in the central regions.

NOMENCLATURE

ϕ : Physical property
ρ : Specific density of air
β : Expansion coefficient
g : Gravitational acceleration
U : Horizontal component of velocity
V : Vertical component of velocity
Γ_ϕ : Diffusion coefficient of ϕ
S_ϕ : Source term of ϕ
X : Horizontal axis or (x)
Y : Vertical axis or (y)
t : Time variable
μ : Molecular viscosity
μ_t : Turbulent viscosity
μ_e : Effective viscosity ($\mu_e = \mu + \mu_t$)
μ : Specific molecular viscosity (μ/ρ)
μ_t : Specific turbulent viscosity (v_t/ρ)
T : Temperature variable
k : Turbulent kinetic energy
ϵ : Dissipative energy
σ_T : Turbulence constant for destruction
σ_K : Turbulence constant for production term k
T_0 : Reference temperature
c_p : Specific heat
a : Molecular thermal diffusivity (= ¯)
λ : Molecular thermal conductivity ($p^* = p/\rho + 3/2k$)
p : Pressure variable
p^* : Total pressure
P_k : Production term
G : Destruction production term
D_j : Local diffusion on j

F_j : Local convection on j
P_j : Local Peclet number on j
U_* : Friction velocity
U^+ : Dimensionless velocity ($U^+ = U/U_*$)
Y^+ : Dimensionless variable ($Y^+ = U\text{-}y/v$)
κ : Von Karman constant ($\kappa = 0.41$)
C_e : Turbulent constant for a smooth wall ($C_e = 9.0$)
ΔT_{pa} : Temperature variation between wall and air ($\Delta T_{pa} = T_p\text{-}T_a$)
S_{ch} : Surface of a room section ($S_{ch} = L^2$)
P_{ch} : Perimeter of a room section ($P_{ch} = 4.L$)
Gr_{cav} : Grashoff number of cavity
Pr : Molecular Prandtl number
D_h : hydraulic diameter of cavity
Ra_{cav} : Rayleigh number of cavity ($Ra_{cav} = Gr_{cav}.\ Pr$)
Re_{cav} : Reynolds number of cavity
Ri_{cav} : Richardson number of cavity
h_{cav} : Convection coefficient
Nu_{cav} : Nusselt number of cavity
T_{pB} : Temperature for measures in lower regions
T_{pH} : Temperature for measures in upper regions

REFERENCES

Brunet, Y., 1989. Contribution to the study of the flow downstream from a T geometry. Ph.D. Thesis, Paul Sabatier University.

Da Graca, G.C., Q. Chen, L.R. Glicksman and L.K. Norford, 2002. Simulation of wind driven ventilation cooling systems for an apartment building in Beijing and Shanghai. Energy Build., 34: 1-11.

Dainese, M.P., 1994. Simulation of incompressible flow of fluid in complex geometry: Contribution to the study of the diagrams of distribution and implicit semi algorithms. Ph.D. Thesis, College of Aeronautics

De Dear, R.J. and G.S. Braer, 2002. Thermal comfort in naturally ventilated buildings: Revisions to ASHRAE standard 55. Energy Buildings, 34: 549-561.

Estivalez, J.L., 1989. Calculation of non stationary flows intern and external by an implicit algorithm of pressure to separate steps. Ph.D. Thesis, University of Toulouse, France

Memeledje, A., 1998. Study of natural air-conditioning by effect of turbulent convection: Modeling and experimentation. Ph.D. Thesis, State University of Cocody, Abidjan

Memeledje, A., 2007. Two-dimensional digital simulation of the turbulent movements of air in a rectangular room of habitat type. Annales de l'université Marien Ngouabi, 8: 123-134.

Memeledje, A., H.C. Boisson, R. Javelas, S. Touré and M. Djoman, 2010. Contribution à l'étude numérique de la climatisation naturelle d'une chambre de type habitat. Rev. CAMES-Série A., 10: 79-84.

Memeledje, A., M. Djoman, M. Begué and S. Touré, 2006. Etude expérimentale des transferts convectifs dans un modèle réduit de type habitation par extraction thermo convective au toit. Rev. Ivoir. Sci. Technol., 7: 11-32.

Patankar, S.V., 1980. Numerical Heat Transfer and Fluid Flow. McGraw Hill, New York, USA.

Rodi, W., 1980. Turbulence models and their application in hydraulics, a state of the art review. The IAHR Section on Fundamentals of Division the Experimental and Mathematical Fluids Dynamics.

Sacre, C., J.P. Millet, J. Gandemer and G. Barnaud, 1992. Guide sur la climatisation naturelle de l'habitat en region tropicale humide. Centre Scientifique et Technique du Batiment.

Sangkertadi, 1994. Contribution a l'etude du comportement thermo aeraulique des batiments en climat tropical humide prise en compte de la ventilation naturelle dans l'evolution du confort. These INSA de Lyon.

Ziskind, G., V. Dubovsky and R. Letan, 2002. Ventilation by natural convection of a one story building. Energy Build., 34: 91-102.